to the field of polymer physics is a gel, provided that its polymeric constituents can be treated as a rigid assembly of nonrotating, nontranslating spherical "blobs" such as those of the Kirkwood–Riseman model.[13]

Acknowledgment. This research was supported by grants from the National Science Foundation.

References and Notes

(1) See, e.g., Landau, L. D.; Lifshitz, E. M. "Fluid Mechanics"; Addison-Wesley: Reading, 1959. Batchelor, G. K. "An Introduction to Fluid Dynamics"; Cambridge University Press: Cambridge, UK, 1967; Chapter 4.
(2) Jeffrey, D. J.; Acrivos, A. *AIChE J.* **1976**, *22*, 417.
(3) Herczyński, R.; Pieńkowska, L. *Annu. Rev. Fluid Mech.* **1980**, *12*, 237.
(4) Pokrovskii, V. N. *Sov. Phys.–JETP (Engl. Transl.)* **1960**, *28*, 339.
(5) Brenner, H. *Annu. Rev. Fluid Mech.* **1970**, *2*, 137.
(6) Arrhenius, S. *Medd. K. V. Nobel Inst.* **1916**, *3*, 13.
(7) Vand, V. *J. Phys. Colloid Chem.* **1948**, *52*, 277.
(8) Mooney, M. *J. Colloid Sci.* **1951**, *6*, 162.
(9) Lamb, H. "Hydrodynamics"; Dover: New York, 1951; p 601.
(10) Lundgren, T. S. *J. Fluid Mech.* **1972**, *51*, 273.
(11) Freed, K. F.; Muthukumar, M. *J. Chem. Phys.* **1978**, *68*, 2088. *Ibid.* **1978**, *69*, 2657. See also Muthukumar, M. *J. Chem. Phys.* **1982**, *77*, 959.
(12) Kapral, R.; Bedeaux, D. *Physica* **1978**, *91A*, 590.
(13) See, e.g., Bohdaneckŷ, M.; Kovâr, J. "Viscosity of Polymer Solutions"; Elsevier: Amsterdam, 1982.

Deformation of Microphase Structures in Segmented Polyurethanes

C. R. Desper,* N. S. Schneider, and J. P. Jasinski†

Organic Materials Laboratory, Army Materials Technology Laboratory, Watertown, Massachusetts 02172

J. S. Lin

National Center for Small Angle Scattering Research, Oak Ridge National Laboratory, Oak Ridge, Tennessee 37830. *Received April 1, 1985*

ABSTRACT: Microstructure deformation in three selected polyurethanes has been studied quantitatively by SAXS during macroscopic tensile strain. The results demonstrate three possible modes of response at the level of the microphase structure: a shear mode, a tensile mode, and rotation or translation of independent particles. In the shear mode, as seen in an amine-cured polyurethane, the hard-segment lamellae tilt away from the stretch direction, while the soft-segment microphase deforms in shear. In the tensile mode, exemplified by a diol-cured polyurethane, the lamellae orient normal to the stretch direction, while the soft-segment microphase deforms in tension. For a triol-cured polyurethane, the local deformation mode is not uniquely determined; results are interpreted in terms of either rotation or translation of microparticles.

Introduction

The elastomeric properties of segmented polyurethanes have long been associated[1-3] with microphase separation, the microphase rich in soft-segment units conferring elastomeric behavior while the microphase rich in hard segments provides physical cross-linking. Bonart[3] studied polyurethane morphology by small-angle X-ray scattering (SAXS) and reported preferred orientation of the periodic microphase structure as a result of tensile stretching. Cooper and co-workers[4-6] measured preferred orientation of the hard and soft segment molecular units within the microphases by infrared dichroism.

Within this context the question of hysteresis must be addressed. In polyurethane elastomers, high levels of long-term residual deformation are commonly observed after removal of stress.[7] For diol-cured elastomers, Estes et al.[4] report residual hard-segment orientation upon removal of applied tensile stress. This orientation hysteresis effect was particularly pronounced[6] in elastomers that totally lack N–H groups to participate in hydrogen bonding. In the opposite extreme, amine-cured polyurethanes, also referred to as poly(urethane ureas), possess two N–H groups per hard-segment repeat compared to one for diol-cured polyurethanes. The amine-cured polyurethanes show[8-13] a greater propensity toward microphase segregation than their diol-cured counterparts, presumably because of the larger number of possible hydrogen bonds between hard-segment chemical groups.

Desper and Schneider[8] have quantitatively characterized microphase segregation in polyurethanes in the undeformed state using methods established[14] for the slit-collimated Kratky SAXS camera. These studies have been extended to investigate the response of polyurethane microstructure to deformation. In the present work, the study of polyurethane microstructure deformation has been undertaken by using a modern SAXS instrument capable of yielding quantitative data in two dimensions. This instrument, the 10-m SAXS camera at the National Cancer for Small-Angle Scattering Research at the Oak Ridge National Laboratory, incorporates pinhole optics and a two-dimensional position-sensitive proportional counter. With the exception of preliminary studies by Abouzahr,[13] this is believed to be the first in-depth study of this kind on polyurethane microstructure deformation.

Experimental Procedures

Sample Preparation. Three polymers representing three distinct classes of polyurethanes were investigated: the first, an amine-cured polyurethane from a series previously characterized[8] in the undeformed state; the second, a triol-cured polymer; the third, a diol-cured polymer. Polymers were synthesized by a two-step process at the compositions given in Table I. For all three polymers the soft segment was poly(tetramethylene oxide) (PTMO) of molecular weight 1000. The hard segment consisted of either toluene diisocyanate (TDI, mixed isomers) or methylenebis(*p*-phenyl isocyanate) (MDI) reacted with either an amine (trimethyl glycol bis(*p*-aminobenzoate), TMAB), a triol (1,1,1-

† Intergovernmental Personnel Act (IPA) fellowship; on leave from the Chemistry Department, Keene State College, Keene, NH 03431.

0024-9297/85/2218-2755$01.50/0

Table I
Polyurethane Composition

	sample descriptor and no.		
	amine cured, PTM/1-1.6	triol cured, TTM/1-3.5	diol cured, MD-85A
diisocyanate			
type	TDI[a]	TDI[a]	MDI[a]
mol	1.6	3.5	1.9
chain extender			
type	TMAB[a]	TMP[a]	BD[a]
mol	0.6	1.67	0.9
soft segment			
type	PTMO[a]	PTMO[a]	PTMO[a]
mol wt	1000	1000	1000
mol	1.0	1.0	1.0
weight fraction, hard segment	0.319	0.473	0.371

[a] TDI, toluene diisocyanate [80:20 mixture of (2,4) and (2,6) isomers]; MDI, methylenebis[*p*-phenyl isocyanate); TMAB, trimethylene glycol bis(*p*-aminobenzoate); TMP, 1,1,1-trimethylolpropane; BD, 1,4-butanediol; PTMO, poly(tetramethylene oxide).

trimethylolpropane, TMP), or a diol chain extender (butanediol, BD), as indicated in Table I. All three polymers were transparent, showing no evidence of crystallinity or macroscopic monomer phase separation. Wide-angle X-ray scattering (WAXS) patterns confirmed the lack of crystallinity. Specimens were available in the form of sheets in thicknesses of 1.33, 1.29, and 1.03 mm, respectively. From these sheets, tensile specimens were cut by using a suitable die to the dimensions of specification ASTM D1708-79, resulting in a sample width of 4.76 mm. A gauge length of 12.7 mm was used in the stretching device.

SAXS Procedures. The Kratky camera was used for detailed characterization of samples in the isotropic state before stretching by using nickel-filtered Cu Kα radiation with a wavelength of 1.5418 Å. The data were corrected for background and for diffuse scattering, in the latter case by using an empirical equation[8]

$$\ln [I_D(\kappa)] = K_1 + K_2\kappa^4 \quad (1)$$

where κ is the scattering variable defined by

$$\kappa = (4\pi/\lambda) \sin \theta \quad (2)$$

In eq 1, I_D is the diffuse scattered intensity, while the constants K_1 and K_2 were determined by fitting the intensity in the 2θ range 8°–16°.

Stretching experiments were run on the Oak Ridge National Laboratory 10-m SAXS camera[15] using X-radiation (monochromated by a graphite crystal) of wavelength 1.5418 Å. For each type of polyurethane, a single sample was mounted in a stretching device in the SAXS camera, and patterns for that sample were obtained in the unstretched state, at 50%, 100%, and 200% elongation, and in the recovered state 5 min after removal of applied stress. The recovered state showed a residual deformation, based on the original sample length, of approximately 10% for the amine- and triol-cured polymers and of 41% for the diol-cured polymer. Data were corrected for detector sensitivity, sample absorption, background, and dark current, and then plotted as two-dimensional contour plots and one-dimensional intensity curves by using the ORNL programs.

Results

From the desmeared Kratky camera SAXS intensity curves for the two samples (see Figure 1) periodicities of 110 and 118 Å are evident for the amine- and diol-cured polymers, respectively, while the intensity curve of the triol-cured polymer decreases monotonically without a diffraction maximum. Parameter values obtained from these data are listed in Table II. Electron-density variance and hard-segment inhomogeneity length are of comparable magnitude for the three samples. Soft-segment inhomogeneity length is greatest for the amine-cured sample, reflecting the higher volume fraction of soft segment. In qualitative terms, all three polymers show extensive microphase separation, but the microphase particles are correlated in position in the amine- and diol-cured polymers, resulting in an interference maximum, while the particles are more randomly placed in the triol-cured polymer.

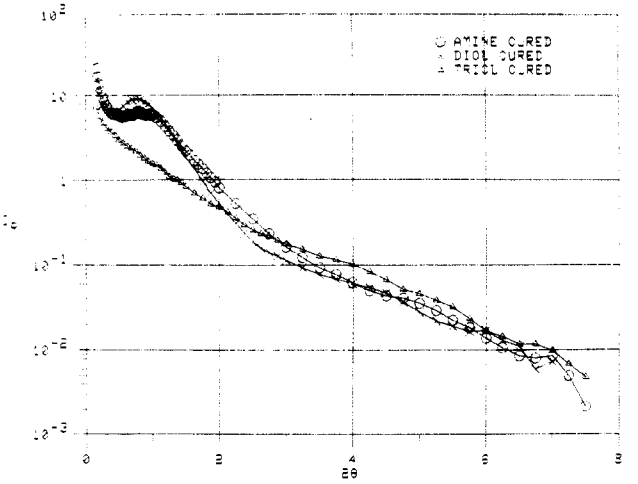

Figure 1. Desmeared Kratky camera SAXS patterns of unstretched polyurethanes. λ = 1.5418 Å; 2θ is in degrees.

Table II
Polyurethane Microstructure Parameters, Isotropic State

	sample descriptor		
	amine cured	triol cured	diol cured
volume fraction HS[a]	0.26	0.38	0.31
repeat period d, Å	110	none	118
HS[a] inhomogeneity length, Å	33	28	43
SS[b] inhomogeneity length, Å	241	46	95
electron-density variance, (mol $e^-/cm^3)^2$	3.30×10^{-3}	2.79×10^{-3}	3.40×10^{-3}

[a] HS, hard segment. [b] SS, soft segment.

Table III
Summary of Stretching Experiment, Amine-Cured Polyurethane

elongation, %	ϕ_{max}[a]	κ_{max}[b]	d_{max}[c]
0	isotropic	0.052	120
50	65°	0.055	114
100	65°	0.055	114
200	65°	0.058	108
10	isotropic	0.055	114

[a] ϕ_{max}, azimuth angle of intensity maximum with respect to stretching direction. [b] κ_{max}, κ value (Å^{-1}) of intensity maximum. [c] d_{max}, corresponding d spacing using Bragg's law.

The essential results of the stretching experiment are shown in the SAXS patterns of Figures 2–4. All three samples show isotropic patterns before stretching, transform to increasingly anisotropic patterns upon stretching, and then return to nearly isotropic patterns when stress is released. However, the diol-cured polymer shows a somewhat elliptical contour pattern after stretching, while the amine- and triol-cured polymer patterns return to circular symmetry. This is consistent with the higher level (41%) of residual elongation in the diol-cured polymer compared to those of the two other polymers. For the amine- and triol-cured polymers the reversibility in the polymer microstructure, as shown in the SAXS patterns, is seen as associated with, and indeed being the cause of, their low hysteresis.

The results of the stretching experiment are examined in more detail in Tables III–V in terms of the scattering

Table IV
Summary of Stretching Experiment, Triol-Cured Polyurethane

elongation, %	intensity ratio I_{90}/I_0 at κ = 0.060 Å^{-1} [a]
0	1.0
50	0.6
100	0.5
200	0.4
11	0.9

[a] I_{90}/I_0, ratio of intensities at ϕ = 90° and 0° at indicated κ (radius) value.

Table V
Summary of Stretching Experiment, Diol-Cured Polyurethane

elongation, %	ϕ_{max} [a]	κ_{max} [b]	d_{max} [c]	R_1 [d]
0	isotropic	0.054	117	
50	0°	0.042	149	17
100	0°	0.043	148	16
200	0°	0.050	127	20
41	near isotropic	0.058	108	

[a] ϕ_{max}, azimuth angle of intensity maximum with respect to stretching direction. [b] κ_{max}, κ value (Å^{-1}) of intensity maximum. [c] d_{max}, corresponding d spacing (Å) using Bragg's Law. [d] R_1, lateral coherent radius of scattering element (Å) after Bolduan and Bear.[18]

variable κ defined by eq 2 and the azimuthal angle ϕ with respect to the stretching direction, which is vertical in Figures 2–4. For the unstretched polymers, the κ dependence of the SAXS intensity (not shown), averaged over all ϕ values, is in agreement with the Kratky camera patterns of Figure 1. At 50%, 100%, and 200% elongation, intensity vs. κ curves were obtained in radial slices (not shown) at various ϕ values; the results on the slice having the higher maximum intensity were entered in Tables III–V.

Although the amine- and diol-cured polymers both show periodicity throughout the stretching experiment, their behavior is markedly different. For the amine-cured polymer, the periodic maximum (Table III) shifts away from the meridian with stretching, developing into a four-point pattern with the periodic maxima tilted at ϕ = 65° for 200% stretch. In the process, a small decrease in period from 120 to 108 Å is observed, returning to 114 Å after release of stress. For the diol-cured polymer (Table V), the periodic maximum is at the meridian (ϕ = 0°) for all elongation values. However, the progression of the period values is quite interesting. As elongation increases from 0% to 50% and 100%, the period increases markedly from 117 to 148–149 Å. When the elongation increased to 200%, the period decreases to 127 Å, then, as the stress is removed, the period decreases even more to 108 Å, in substantial agreement with the original period.

For the triol-cured polymer the SAXS pattern becomes increasingly anisotropic with elongation, with enhanced intensity in the equatorial zone and depleted intensity at the meridian, showing no periodicity at any level of elongation. As a measure of anisotropy, the ratios of the intensities at ϕ = 0 and 90° for a fixed κ value of 0.060 Å^{-1} are given in Table IV. This ratio decreases from 1 to 0.4 with increasing elongation, returning to 0.9 with release of the stress.

The orientation dependence of the scattering pattern is examined in the ring plots of Figures 5–7. These plots show the angular intensity dependence in rings of fixed κ values around the center of the diffraction patterns. The ring plots for the amine-cured sample (Figure 5) at κ values corresponding to the radial maxima exhibit the four-point scattering pattern, with the maxima corresponding to

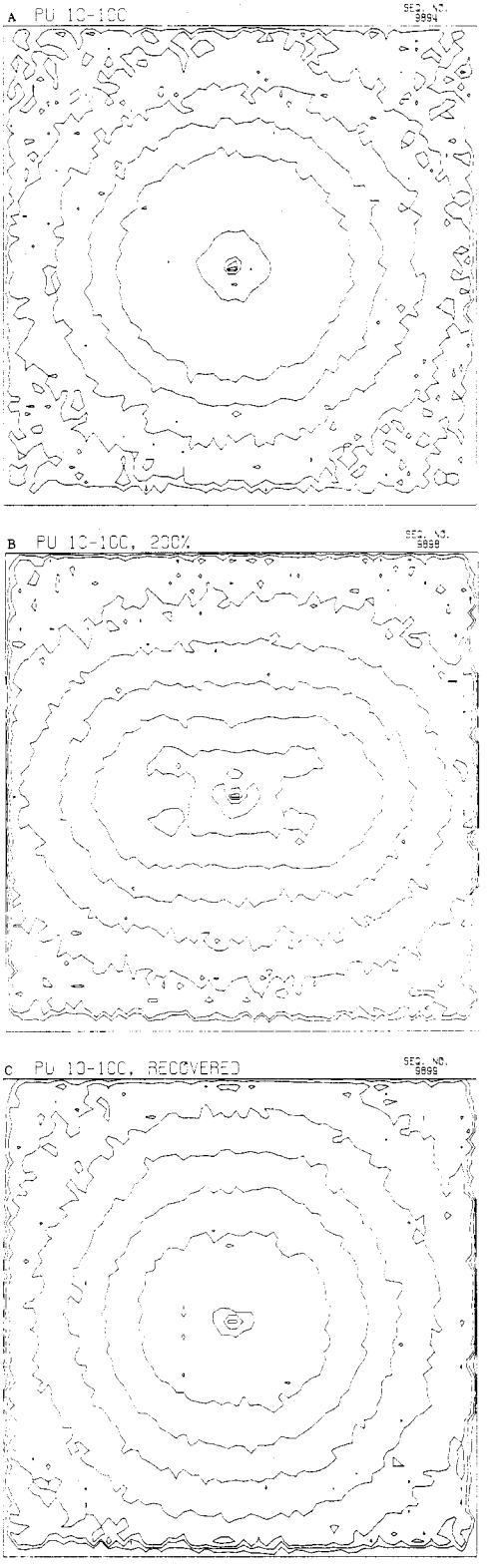

Figure 2. Pinhole SAXS patterns of amine-cured polyurethane PTM/1-1.6: (a) unstretched; (b) stretched 200%; (c) recovered. Approximate κ range: −0.17 to +0.17 Å^{-1} horizontally and vertically.

preferred azimuth angles of ϕ = ±65° and ±115°, at 50%, 100%, and 200% stretch. It is particularly notable that the four-point nature of the patterns is evident in the ring plots at 50% and 100% stretch, since this is not evident in the corresponding contour plots (Figure 2b,c). The ring patterns (Figure 5) show a distinct four-point pattern at the 50% stretch level, which becomes pronounced in terms of the ratios of maxima to minima in the ring pattern,

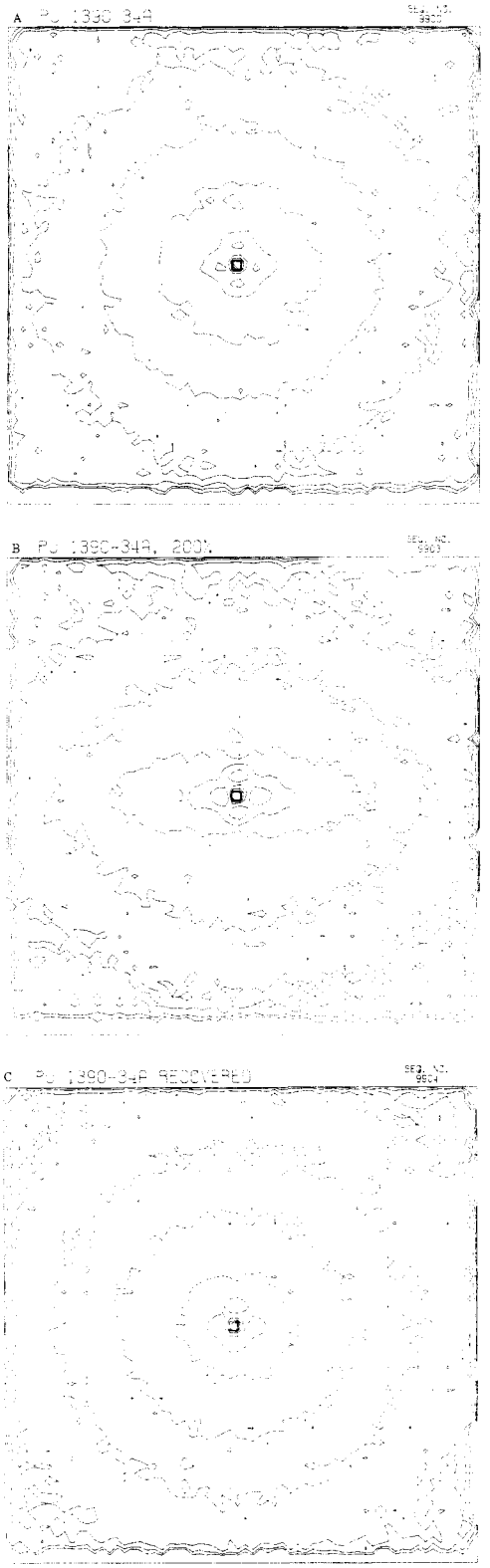

Figure 3. Pinhole SAXS patterns of triol-curved polyurethane TTM/1-3.5: some strain values and κ range as in Figure 2.

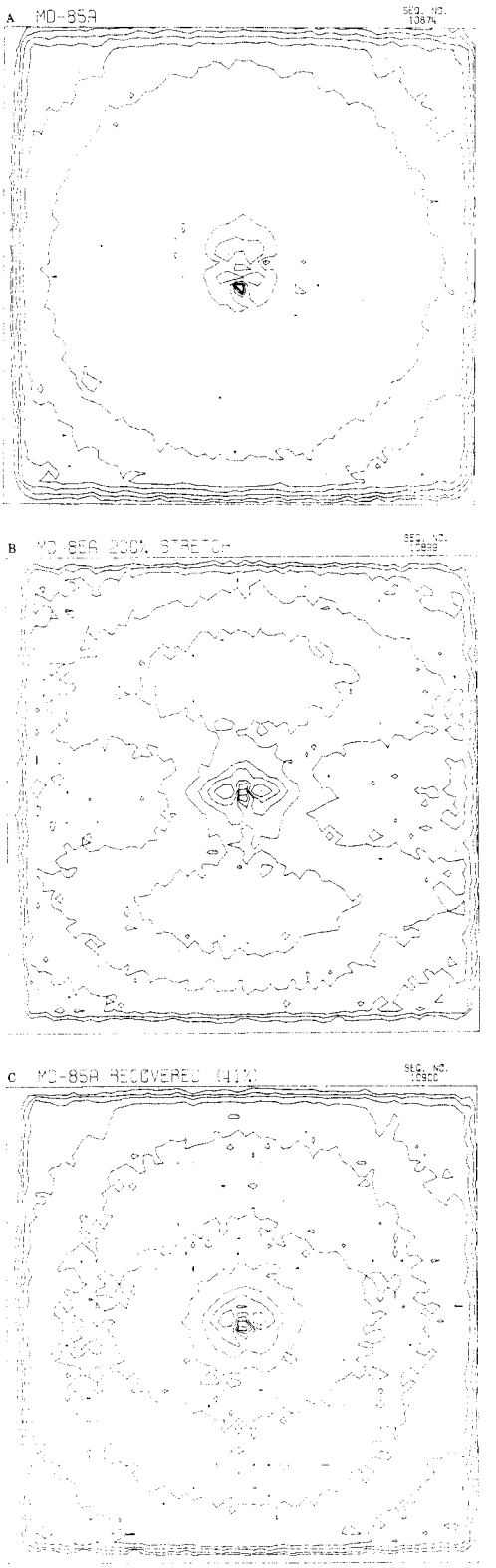

Figure 4. Pinhole SAXS patterns of diol-cured polyurethane MD-85A: same strain values as in Figure 2. Approximate κ range: -0.09 to $+0.09$ Å^{-1} horizontally and vertically.

without noticeable change in the position of the ring maxima.

The ring patterns for the triol-cured specimen (for which there is no radial maxima) were taken at κ value of 0.060 Å^{-1}, comparable to the radial maxima of the amine- and diol-cured polyurethanes (see Figure 6). In this case the stretched specimens showed twofold symmetry about the center of the SAXS patterns, with maxima corresponding to $\phi = \pm 90°$, i.e., at the equatorial position. The ring patterns of the unstretched state and of the recovered specimen show only a small ϕ dependence; the latter indicates the reversibility of the microstructure deformation process.

The ring patterns for the diol-cured specimen, again taken at κ values corresponding to the radial maxima, show twofold symmetry about the center of the SAXS patterns at 50%, 100%, and 200% stretch (see Figure 7). In these cases the maxima correspond to ϕ values of 0 and 180°; i.e. they are meridional maxima. One striking aspect of

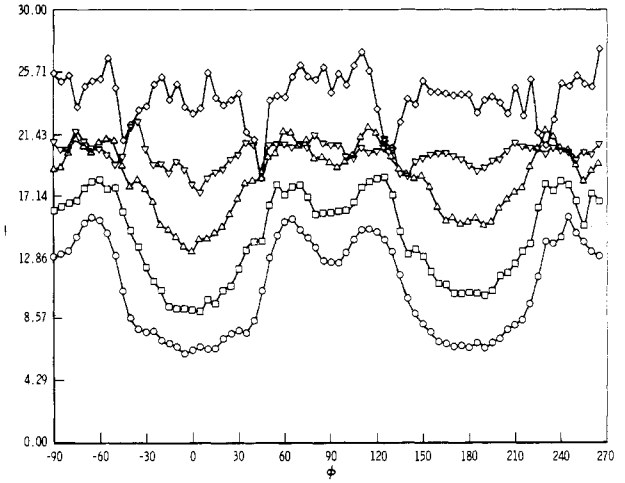

Figure 5. Ring plots for the amine-cured polyurethane derived from SAXS data of Figure 2 at fixed radius (κ) values corresponding to the κ_{max} values given in Table III: (◇) 0%; (△) 50%; (□) 100%; (○) 200%; (▽) recovered.

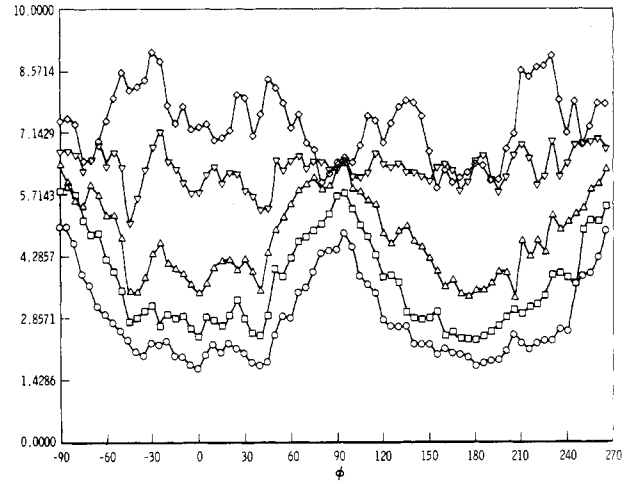

Figure 6. Ring plots for the triol-cured polyurethane derived from SAXS data of Figure 3 at fixed raidus (κ) value of 0.060 Å^{-1}. Symbols have same designations as in Figure 5.

these ring patterns, which will be discussed at a later point, is that the ring maxima corresponding to 50%, 100%, and 200% stretch are quite broad.

Discussion

Three different modes of deformation of polyurethane microstructures are evident from the SAXS data. For the amine-cured polyurethane there is evidence that the macroscopic tensile deformation results in shearing at the microstructure level. At 50% elongation, the lowest stretch level, the periodic interference maximum has completely vanished in the meridional ($\phi = 0°$) direction. This part of the SAXS pattern remains depleted of intensity at higher elongations, but the periodic maximum returns when stress is removed. Those lamellar structures that, prior to stretching, were oriented normal to the stretch direction undergo interlamellar shear in the soft-segment microphase to tilt away from the stretch direction. Lamellar structures originally tilted at an angle to the stretch direction tilt to higher angles (but not to $\phi = 90°$) with stretching, as shown in Figure 8, resulting in a shortened periodic maximum in regions away from the meridian. Finally, at 200% elongation sufficient lamellar structures have tilted to a preferred $\phi = 65°$ angle to give a discernible four-point pattern.

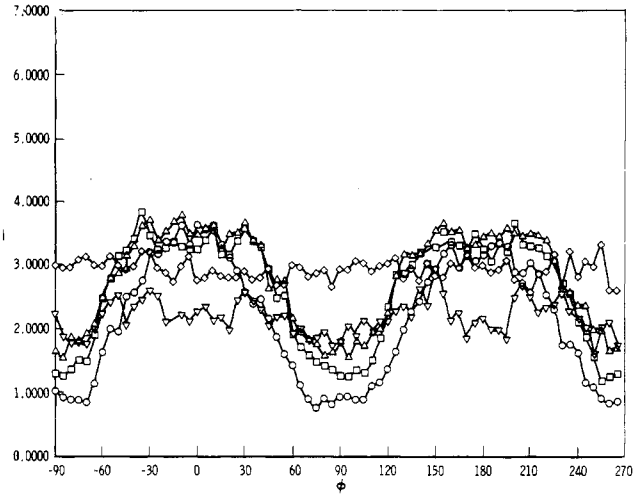

Figure 7. Ring plots for the diol-cured polyurethane derived from SAXS data of Figure 4 at fixed radius (κ) values corresponding to the κ_{max} values of Table V. Symbols have same designations as in Figure 5.

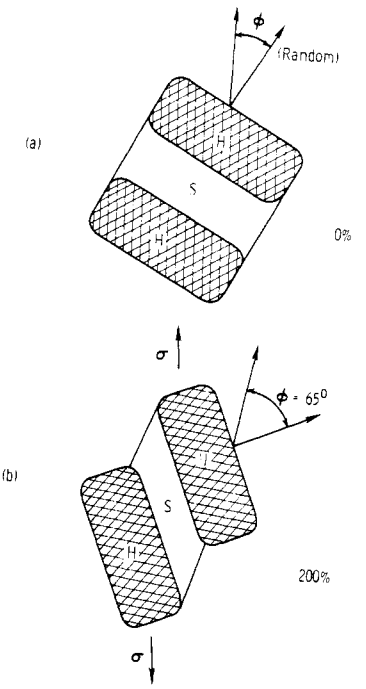

Figure 8. Tensile deformation resolved into interlamellar shear at the microdomain level.

The diol-cured polyurethane illustrates the second possible mode of deformation, in which the macroscopic tensile deformation is translated into tensile deformation of the microstructure, as illustrated in Figure 9. At 50% elongation, the interference maximum is strengthened in the meridian and weakened at the equator. Concurrently, the original 117-Å periodic spacing increases to 149 Å at the meridion. The two observations clearly indicate a turning of the periodic direction of the lamellar structures toward the stretch direction, accompanied by extension of the soft-segment phase in tension to increase the period in the stretch direction. With extension to 100% the period is unchanged, while the period decreases to 127 Å at 200% elongation. This is taken to indicate the breakup of the hard-segment phase into smaller chunks that act less like a continuous phase and more likely very small isolated particles. Such a deformation of the hard-segment phase must be viewed as a plastic process, not reversible except possibly after a long period of time. Indeed, this

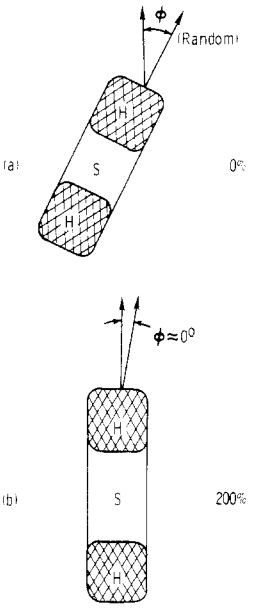

Figure 9. Tensile deformation resulting in tensile strain at the microdomain level.

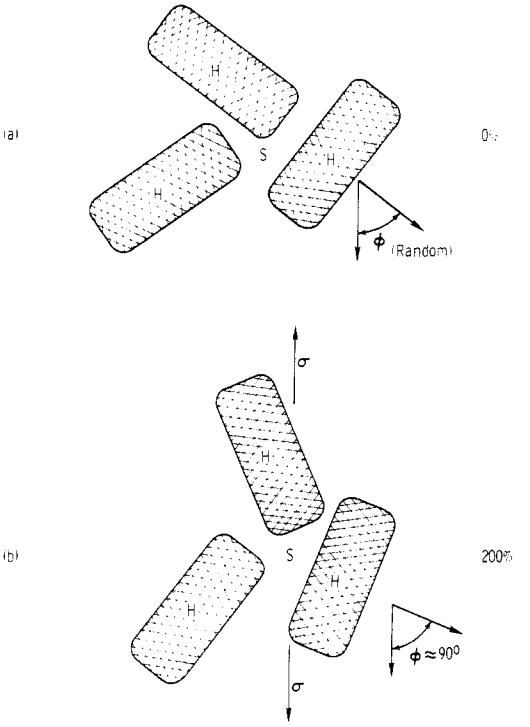

Figure 10. Tensile deformation resulting in rotation of independent particles at the microdomain level.

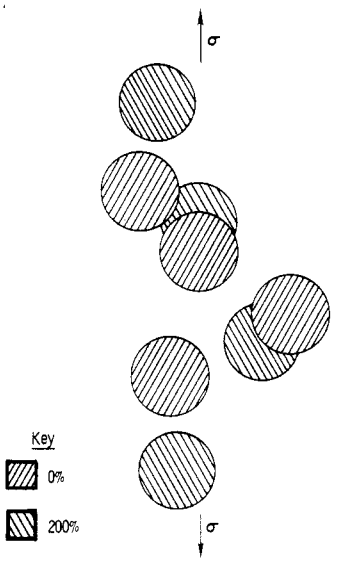

Figure 11. Tensile deformation resulting in positional translation of an array of randomly placed spheres at the microdomain level.

disruption of the hard-segment-phase continuity is probably the origin of the stress-softening effect in cyclic loading, as described by Keltenborn and Soon[16] and Godovsky.[17]

In this context it is instructive to examine the tangential extension of the meridional maxima for the diol-cured polymer. Examination of the contour patterns (see Figure 4) suggests that the meridional maximum has the form of a horizontal streak rather than an arc. Consequently, the tangential spread of the pattern may result from the limited lateral length of the scattering elements rather than from distribution in orientation. Bolduan and Bear[18] first treated this problem in terms of the meridional reflections of collagen and related the tangential spread ξ_n of SAXS intensity for the nth meridional reflection (in reciprocal space units) to the coherent lateral radius R_n of the scattering elements. The relationship given by Bolduan and Bear is

$$R_n = \{\ln 2/[\pi^2\nu^2(\xi_n^2 - \xi_0^2)]\}^{1/2} \quad (3)$$

where n is the order of the reflection (1 in the present case), ν is the reciprocal of the X-ray wavelength, and ξ_0, the lateral spread of the primary beam, is neglected in the present context. Hess and Kiessig[19] and Statton[20] later applied this method of interpretation to synthetic polymers. The results of this treatment, where applicable, are entered in the final column of Table V. The R_1 values obtained are in the range of 16–20 Å, corresponding to cylinder diameter values of 32–40 Å. These small diameter values, compared to the repeat periods in the 100–150-Å range, support the contention that the hard-segment microphase particles are cylindrical rather than disk-shaped in the diol-cured polymer and also may have undergone lateral breakup in the stretching process.

Finally, in the case of the triol-cured polyurethane, no periodicity effects are involved. The high level of electron-density variance (Table II) indicates that microphase particles exist in the triol-cured polyurethane. However, this polymer does not develop a repeating structure of sufficient regularity to give an interference maximum in either the isotropic or deformed states. Nonetheless, the irregular microstructural elements present in this material give increasingly anisotropic scattering patterns as the sample is deformed. Summerfield and Mildner have demonstrated[21] that elliptical symmetry with respect to azimuth angle ϕ in the SAXS pattern does not imply that the scattering centers themselves are elliptical; it only implies that the average inertial distance due the effects of size, shape, position, and orientation must exhibit elliptical symmetry with respect to the azimuthal angle. Thus, at least two interpretations of the data are possible, each having equal validity in terms of SAXS theory. On the one hand, one could interpret the shift of the SAXS intensity to the equatorial zones to indicate that the elementary particles of the microstructure is elliptical in shape and that the long axes of these elementary particles turn toward the stretch direction (see Figure 10). On the other hand, an equally valid interpretation, depicted in Figure 11, would consist of a microstructure of isotropic particles that respond to stretching by changing their displacements with respect to each other. The SAXS data

do not distinguish among these two possibilities or a combination of the two effects.

The low level of hysteresis in the amine- and triol-cured polyurethanes is related to the resistance to plastic deformation of the hard-segment microparticles. In the case of the triol-cured polymer, the covalent cross-links between chains prevent chain slip from occurring in the hard-segment phase. For the amine-cured polymer, the hydrogen bonding within the hard-segment phase between the C=O and N—H groups of adjacent molecules serves the same function. Sung et al.[10] and Wilkes[12] attribute the high degree of microphase segregation in amine-cured polyurethanes to a higher level and strength of hydrogen bonding, each C=O group of the urea linkage in the hard segment participating in hydrogen bonds with N—H groups from two adjacent molecules. Thus amine curing, which results in a urea linkage, provides twice as many moles of N–H for hydrogen bonding compared to diol curing and also results in hydrogen bonding of greater strength per bond. These factors tend to reduce hysteresis by preventing the plastic deformation and breakup of the hard-segment microphase particles.

Summary

The elastomeric properties of segmented polyurethanes have long been associated with microphase separation, the microphase rich in soft-segment units conferring elastomeric behavior while the microphase rich in hard segments provides physical cross-linking. The behavior of such microstructures in a variety of polyurethanes under conditions of macroscopic tensile loading have been examined quantitatively by SAXS, using the 10-m camera at the Oak Ridge National Laboratory. The data obtained offer both a qualitative and a detailed description of the effect of the deformation process at the microphase level. Depending upon the type of polyurethane, the microstructure may deform by either local shearing or local tensile deformation of the soft-segment regions. The mechanism operating for a particular polyurethane depends upon the shape and structural integrity of the hard-segment domain particles.

The shearing mechanisms, which predominates for disk-shaped hard-segment particles with good structural integrity, results in tilting of the hard-segment lamellae away from the direction of elongation. Such behavior is typified by a four-point SAXS pattern with maxima at 65° to the stretch direction and is associated with a lower level of mechanical hysteresis.

In the tensile mechanism, in contrast, the hard-segment particles respond like cylinders in which the thickness and diameter are comparable. In this case the repeating direction of the microstructure, which is along the cylinder axis, turns toward the stretch direction, resulting in a two-point SAXS pattern with maxima parallel to the stretch direction. The SAXS repeat period is seen to increase in the early stages of deformation; however, between 100% and 200%, a significant decrease in long period has been seen. The data are taken to indicate the breakup of the hard-segment phase into smaller chunks, compromising the physical cross-linking effect. Such behavior is found to be associated with a higher level of mechanical hysteresis.

In a third class of polyurethanes, characterized by chemical cross-linking within the hard-segment phase that precludes the formation of a regularly repeating structure, interpretation of the deformation behavior is more ambiguous, since the shape of the microphase particles is not established. If elongated particles were present, the results could be interpreted to indicate the rotation of the long axes of the particles toward the stretch direction. A similar shift in intensity to the equatorial position with stretching could result, however, from the simple translation of positions of an array of spheres.

The results presented here are based on experiments with a very limited number of polymers and should not be taken as characteristic of broad classes of polyurethanes; details of chemical composition and morphology may well influence the mode of response of a particular polymer. Further studies are in progress involving a wider variety of polyurethanes.

Acknowledgment. We wish to express our gratitude to Dr. Richard Baron of Polaroid Corp. and to Dr. Kurt C. Frisch of the University of Detroit for providing polymer samples. We also wish to acknowledge our debt to the staff at the Oak Ridge National Laboratory, whose efforts made available the 10-m SAXS instruments and the programs for data acquisition and data reduction. In particular we offer our thanks to the National Science Foundation and the Department of Energy, whose funding support provided these facilities and capabilities, which were indispensible to the success of this study.

References and Notes

(1) Cooper, S. L.; Tobolsky, A. V. *J. Appl. Polym. Sci.*, **1966**, *10*, 1837.
(2) Clough, S. B.; Schneider, N. S.; King, A. O. *J. Macromol. Sci., Phys.* **1968**, *B2*, 641.
(3) Bonart, R. *J. Macromol. Sci., Phys.* **1968**, *B2*, 115.
(4) Estes, G. M.; Seymour, R. W.; Cooper, S. L. *Macromolecules* **1971**, *4*, 456.
(5) Seymour, R. W.; Allegrezza, A. E., Jr.; Cooper, S. L. *Macromolecules* **1973**, *6*, 896.
(6) Allegrezza, A. E., Jr.; Seymour, R. W.; Ng, H. N.; Cooper, S. L. *Polymer* **1974**, *15*, 433.
(7) Hepburn, C. "Polyurethane Elastomers"; Applied Science: New York, 1982; pp 56–61, 249–253.
(8) Desper, C. R.; Schneider, N. S. In "Polymer Alloys III"; Frisch K.; Klemper, D., Eds.; Plenum Press: New York, 1983; pp 233–251.
(9) Paik Sung, C. S.; Hu, C. B.; Wu, C. S. *Macromolecules* **1980**, *13*, 111.
(10) Paik Sung, C. S.; Smith, T. W.; Sung, N. H. *Macromolecules* **1980**, *13*, 117.
(11) Wang, C. B.; Cooper, S. L. *Macromolecules* **1983**, *16*, 775.
(12) Wilkes, G. L.; Abouzahr, S. *Macromolecules* **1981**, *14*, 212.
(13) Abouzahr, S. Ph.D. Thesis, Chemical Engineering Department, Virginia Polytechnic Institute and State University, Blacksburg, VA, 1981.
(14) Koberstein, J. T.; Morra, B.; Stein, R. S. *J. Appl. Crystallogr.* **1980**, *13*, 34.
(15) Hendricks, R. W. *J. Appl. Crystallogr.* **1978**, *11*, 15.
(16) Keltenborn, J. C.; Soong, D. S. *Polym. Eng. Sci.* **1982**, *22*, 654.
(17) Godovsky, Yu. K. *Makromol. Chem., Suppl.* **1984**, *6*, 117.
(18) Bolduan, O. E. A.; Bear, R. S. *J. Polym. Sci.* **1951**, *6*, 271.
(19) Hess, K.; Kiessig, H. *Kolloid-Z.* **1953**, *130*, 10.
(20) Statton, W. O. *J. Polym. Sci.* **1958**, *28*, 423.
(21) Summerfield, G. C.; Mildner, D. F. R. *J. Appl. Crystallogr.* **1983**, *16*, 384.